Electrostatic removal of lithium fluoride from field-emitter tips at elevated temperatures

J. A. Panitz
High-Field Consultants, Inc., Edgewood, New Mexico 87015-9750

(Received 24 March 1994; accepted 24 May 1994)

The electrostatic removal of lithium fluoride (LiF) from field-emitter tips has been visualized at elevated temperatures in the transmission electron microscope (TEM). The apex of a field-emitter tip coated with ~1500 Å of LiF provides a unique substrate for observing the removal process in the TEM in real time, and its curvature generates the required electrostatic field strength. The influence of the imaging electron beam on coating morphology has been visually assessed. A LiF coating can tolerate an electron dose of ~2000 $e^-/\text{Å}^2$ at room temperature without visible damage (at a resolution of 5 Å). At elevated temperatures a higher dose can be tolerated before visible damage is observed. Removal of LiF coatings at room temperature occurs at 18 MV/cm. At 800 °C piecewise removal of the coating occurs at 9 MV/cm. Synergistic effects of the electron beam and the electrostatic field on the removal of the coating were not observed. The removal of LiF at any temperature is attributed to field-induced fatigue stress of the coating. Field desorption does not appear to play a significant role in the removal process. Implications for the production of ions from lithium fluoride thin films exposed to high electric fields (in laboratory experiments and in particle beam fusion accelerators such as PBFA II) are discussed.

I. INTRODUCTION

The desorption of alkali halide crystals at elevated temperatures in high electric fields is of intrinsic interest.[1–3] Field desorption of lithium fluoride (LiF) is of practical importance at any temperature because it is the mechanism assumed to produce intense Li^+ ion beams in inertial confinement fusion accelerators.[4,5] This investigation provides the first direct visual examination of the process that removes a LiF coating from a metal surface in an electrostatic field. The transmission electron microscope (TEM) was used to observe the morphology of a LiF coating as a function of temperature, in real time, on a field-emitter tip during the removal process.

The apex of a field-emitter tip coated with ~1500 Å of LiF provides a unique substrate for observing the removal process in the TEM, and its curvature generates the required electrostatic field strength. Field enhancement produces a field strength of 1 MV/cm at the tip apex when the tip is biased to a few hundred volts. Field-emitter tips are prepared by electropolishing a 0.006 in. diam wire of the selected material to the required dimensions.[6] For example, tungsten tips are formed by electropolishing in 1*N* NaOH at a few volts ac while type 304 (stainless steel) tips are formed by electropolishing in Electroglo 300 at a few volts dc.[7] After etching, a tip is spot welded to a 0.008 in. diam molybdenum wire loop and placed in an oil-free vacuum chamber that is pumped to a base pressure of $\sim 10^{-9}$ Torr. The apex radius of the tip is increased to the required dimension (and made smooth on a nanometer scale), by heating the tip to a temperature of ~80% of its melting point for several seconds. At this temperature, self-diffusion of surface atoms proceeds rapidly, and forms the tip apex into an approximately spherical contour of minimum free energy.[8] The tip is heated by passing a known current through the loop. Thermal conduction heats the tip apex to the required temperature.

II. ELECTRIC FIELD CALIBRATION

Field calibration requires a knowledge of the proportionality factor between the electric field at the tip apex and the potential difference V between the tip and a counterelectrode (at ground potential) placed several millimeters from the apex. The electric field at the tip surface varies from its apex to its shank in a manner that depends on the exact shape of electrodes and their spatial configuration. The average electric field strength F at the apex of a clean field-emitter tip is given by

$$F = V/\kappa R, \tag{1}$$

where κ is a geometric factor that depends on the tip shape and the electrode geometry, and R is the radius of curvature of the tip apex. κR can be determined for each tip from a Fowler–Nordheim analysis of its electron emission characteristics in high vacuum. During a Fowler–Nordheim analysis the tunneling current I drawn from the tip apex is measured as a function of the applied voltage V. Fowler–Nordheim analysis assumes that the tunneling barrier at the tip apex (i.e., the average work function ϕ) is known and remains constant during the $I-V$ measurements. $I-V$ measurements are made quickly at a pressure of 10^{-9} Torr to ensure that the work function will not change as gas phase contaminants are adsorbed onto the tip apex during the measurements. Adsorbed contaminants are removed from the tip apex prior to the measurements by heating the tip to ~800 °C. After the tip cools to room temperature (~30 s) and a base pressure of $\sim 10^{-9}$ Torr is reestablished, $I-V$ measurements are taken. To ensure the field calibration applies to the TEM experiments, an electrode geometry is chosen which closely approximates the actual geometry of the tip and the surrounding TEM stage at ground potential. The enhancement factor κR is found from the Fowler–Nordheim equation:

 0734-211X/94/12(5)/2889/5/$1.00

$$I/V^2 = a\exp(-b'\phi^{3/2}/V),$$

$$a = (A)6.2\times10^{-6}(\mu/\phi)^{1/2}(\mu+\phi)^{-1}(\alpha\kappa R)^{-2},$$

$$b' = 6.8\times10^{7}\alpha\kappa R,$$

where A is the total emitting area, α is the Nordheim image-correction term, and μ is the Fermi energy of the metal. A plot of $\ln(I/V^2)$ vs $1/V$ is linear, with a slope

$$m = -b'\phi^{3/2} = -6.8\times10^{7}\alpha\kappa R\phi^{3/2}. \tag{1}$$

An iterative procedure is used to find the enhancement factor.[9] The procedure is outlined below:

(1) As a first approximation to κR, set $\alpha=1$ and find κR from Eq. (1) using the measured slope and the work function of the clean tip apex.
(2) Use the value of κR found in step (1) to find the average field from $F_{\text{average}} = V_{\text{average}}/\kappa R$.
(3) Find a new value of α using the approximation[9] $\alpha=(1-y)^{1/2}$, where $y=3.8\times10^{-4}F^{1/2}/\phi$.
(4) Repeat steps (1)–(3) until the new and the previous value of α agree to a precision of 0.1%. The iteration converges rapidly (typically within ten cycles).

After an analysis of 24 tips was completed, a LiF coating was applied simultaneously to the tips (12 tungsten and 12 CRES) in a turbopumped (oil-free) vacuum evaporator at a pressure of 10^{-6} Torr. A tungsten boat was filled with reagent grade LiF, covered by a removable shutter, and outgassed at dull red heat. After the pressure returned to its base value of 10^{-6} Torr (~30 s), the shutter was opened, the boat temperature was increased, and the tips were coated with LiF. A quartz disk placed in the plane of the tips recorded an interference pattern that reflected the thickness of the film and the spatial uniformity of the deposition process. After ~10 s the shutter was closed, the boat was allowed to cool to room temperature (~200 s), and the evaporator was opened to air.

A. Current density measurements

An upper limit on the current density that can be used for imaging lithium fluoride in the TEM is set by the maximum dose of electrons the coating can tolerate without a visible change in morphology (i.e., at a resolution of 5 Å). This is called the "damage threshold," D_T, of the coating. The beam current at the tip apex I is measured by placing a Faraday collector at the eucentric imaging position of the microscope (normally occupied by a field-emitter tip) as shown schematically in Fig. 1. The corresponding current density is

$$J_E = 4IM^2/\pi D^2,$$

where D is the diameter of the electron beam as measured on the fluorescent screen of the microscope at a magnification M. Table I summarizes the results of the current density measurements.

Experimentally, the damage threshold for a LiF coating is exceeded when the coating is subjected to a current density $J_E \sim 0.07$ A/cm^2 for time periods greater than 45 s. That is,

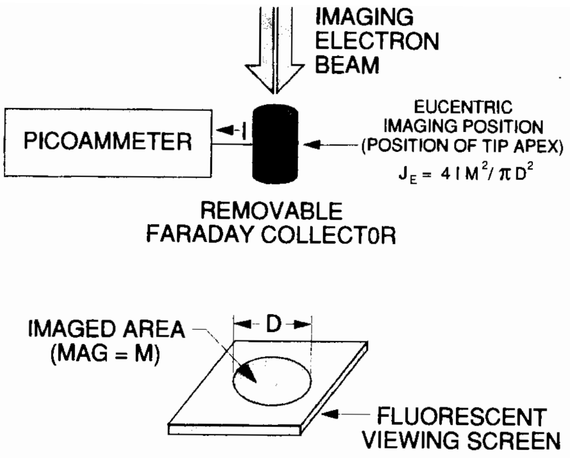

FIG. 1. Method used to determine the current density of electrons, J_E, at the apex of a field-emitter tip during TEM imaging.

$$D_T = (0.07\ \text{C/s cm}^2)(45\ \text{s})(10^{-16}\ \text{cm}^2/\text{Å}^2)/(1.6\times10^{-19}\ \text{C}/e^-) = 1969\ e^-/\text{Å}^2.$$

This result is consistent with the damage threshold observed for other thin insulating films in the TEM, and well above the damage threshold of ~0.5 $e^-/\text{Å}^2$ observed when a single organic molecule is imaged in the TEM without structural alteration at a resolution of 0.5 Å.[10]

If the electron dose is kept below ~10^4 $e^-/\text{Å}^2$, the damage to the coating is marginal. If the dose exceeds ~10^5 $e^-/\text{Å}^2$ the LiF coating appears to "boil," and its entire morphology is altered. These effects are illustrated in Fig. 2. Morphological changes in the coating do not appear to be thermally induced because the rate of thermal drift observed in the image is comparable to the drift normally observed in a TEM image. A simple calculation of the thermal energy which must be dissipated under these imaging conditions supports this conclusion. The energy loss in the coating, $dE/dx = 5.3\times10^6$ eV/cm. At a current density of 0.07 A/cm^2 the energy deposition rate is 3.7×10^5 J/cm^3 s. Since the volume of a tip is ~10^{-15} cm^3, the energy which must be dissipated as heat in the tip shank during the imaging process is only 10^{-10} J/s.

The damage threshold imposes a limit on the number of LiF images that can be recorded on photographic film. Experimentally, one finds that adequate image contrast requires a minimum exposure time of ~2 s at a current density of

TABLE I. JEOL 2000CX TEM current density (J_E) as a function of imaging parameters.

Spot	CA (μm)	Magnification	I (nA)	J_E (A cm^2)
1	None	100×10^3	560	31.7
1	None	50×10^3	560	7.90
1	120	100×10^3	99.8	5.60
1	120	50×10^3	99.8	1.40
3	120	50×10^3	18.4	0.41
3	40	100×10^3	2.21	0.19
4	120	50×10^3	3.00	0.07
5	120	50×10^3	0.50	0.01

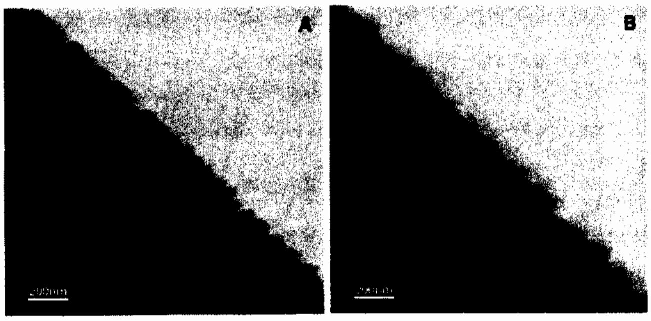

FIG. 2. Electron beam induced damage to a lithium fluoride coating on a field-emitter tip during TEM imaging. (A): Slight damage at $<10^4\ e^-/\text{Å}^2$ (TEM micrograph 2214). (B): Severe damage at $10^5\ e^-/\text{Å}$ (TEM micrograph 2217).

0.07 A/cm^2. If 3 s is taken as the minimum beam time required to prepare for an exposure (focusing, etc.), the total beam time per exposure is 5 s. This implies that a total of nine images can be recorded on photographic film before the damage threshold is reached. To circumvent this difficulty, a low light level charge-coupled device imaging system was used which can record a TEM image on videotape, in real time, at a somewhat lower current density ($\sim$0.02 A/cm^2). The imaging system provided continuous, videotape documentation of the desorption experiments. In addition, the voltage applied to the tip was monitored and superimposed on the videotape image to record the field strength at the tip apex as a function of time. The experimental apparatus is shown, schematically, in Fig. 3.

III. EXPERIMENTAL PROTOCOL

A TEM goniometer stage was constructed for these experiments. Each leg of the molybdenum wire loop that supported a tip made a friction fit with a nickel wire electrode located inside the bore of a dual-bore alumina tube. The tip could be heated by conduction when the molybdenum wire loop was heated resistively (by passing a constant current

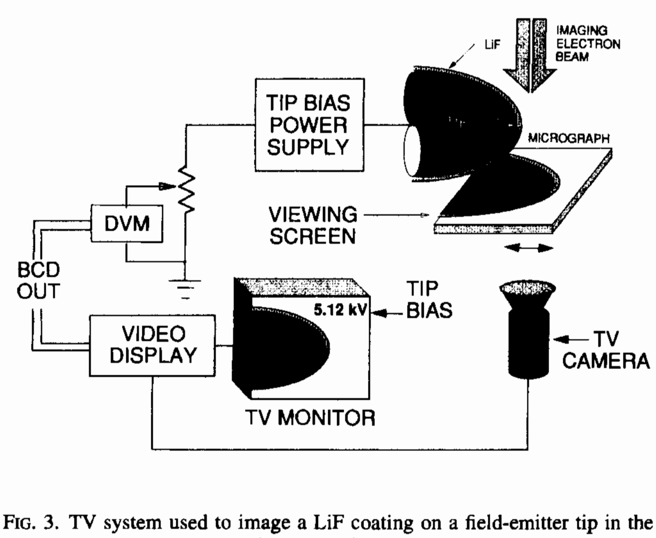

FIG. 3. TV system used to image a LiF coating on a field-emitter tip in the TEM. A videotape recorder (not shown) records the TEM images in real time.

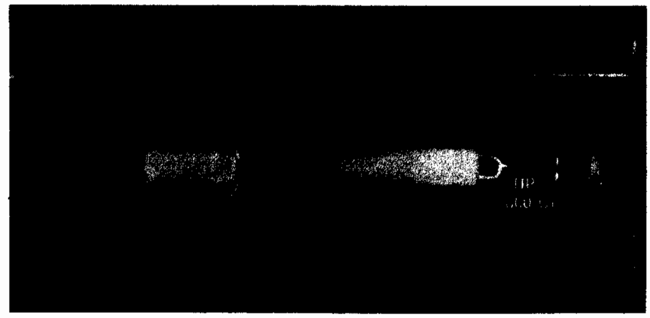

FIG. 4. TEM goniometer stage used to visualize lithium fluoride coatings on field-emitter tip subjected to high temperatures. A field-emitter tip can be heated to a temperature above 800 °C while the tip is biased to a voltage of several kV. Thermal drift requires constant manipulation to keep the image of the tip apex in focus and centered in the field of view of the microscope at elevated temperatures.

through the nickel wire electrodes). A tip could be heated to a maximum temperature of 850 °C while biased to a maximum voltage of $\sim$8 kV (with respect to ground). The goniometer stage is shown in Fig. 4.

A temperature calibration was performed on each tip after an experiment without changing the position of the tip in the goniometer stage. The tip temperature was measured by an optical pyrometer. Temperatures below 700 °C could not be detected by the pyrometer, but were estimated by assuming a linear relation between loop current and temperature. If zero current was assumed to correspond to room temperature (20 °C), then the temperature calibration data extrapolated to a reasonable temperature of $\sim$250 °C at a heating current of 0.5 A.

An experimental protocol was designed to identify synergistic effects of the applied field and the imaging electron beam at room temperature. Recalling that field strengths are calculated from $F=V/\kappa R$ (with κR measured for the *uncoated* tip apex):

(1) The field at the tip apex is increased to $F=10$ MV/cm while imaging.
(2) The tip is positioned just outside of the electron beam, and (a) the apex field is increased by $\Delta F=1.5$ MV/cm; (b) the apex field is decreased by $\Delta F=1.5$ MV/cm.
(3) The tip is returned to its original position in the electron beam, and the apex field is increased to $F=F+\Delta F$ while imaging.
(4) Steps (1)–(4) are repeated until the LiF layer is removed from the tip apex.

The appearance of the desorption process was identical from tip to tip and always progressed in a similar way as a function of field strength. As the field strength was increased to $\sim$15 MV/cm either the coating was removed from the tip apex, or a significant portion of the coating was removed. A further increment in field strength (ΔF) removed the remaining coating at the apex except for a small, residual layer that always displayed a needlelike morphology. The TEM micrographs in Fig. 5 document this phenomena. As the field

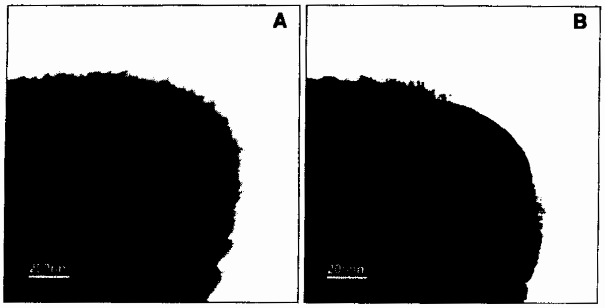

FIG. 5. Room temperature removal of LiF from a field-emitter tip. (A) Undamaged coating (TEM micrograph 2140). (B) After applying a field of 18.7 MV/cm. Note the "needlelike" residual layer remaining at the tip apex (TEM micrograph 2141).

strength was increased further, the coating on the shank of the tip was progressively removed, commencing near the tip apex (where the highest field occurs).

Within experimental error, the presence of electron beam irradiation had no effect on the desorption field strength, or on the appearance of the desorption process. The results of the room temperature experiments are summarized in Table II.

Two different experiments were performed to investigate the effect of applying an electric field to the tip apex at elevated temperatures. An imaging current density $J_E = 0.07$ A/cm^2 was chosen for these experiments. Electron beam damage was not observed at this current density when the temperature of the coating was $\geqslant 300$ °C, presumably because the coating was being annealed as damage occurred. Two different experiments were performed:

(I) The field at the tip apex was increased to ~6 MV/cm, and then the temperature of the tip was increased until a change in the morphology of the coating was noted.

(II) The temperature of the tip was increased to 830 °C, and then the field at the tip apex was increased until a change in coating morphology was observed.

The experiments at elevated temperature were similar to their counterparts at room temperature in that the presence of electron beam irradiation appeared to have no effect on the desorption properties of the LiF coating. However, above 800 °C (at zero field) the coatings become uniformly less electron opaque with time, a phenomenon that was associated with thermal evaporation of the coating. The visual appearance of the process that leads to the removal of the coating at elevated temperatures is similar to the process observed at room temperature in that the coating is removed

TABLE II. Summary of experiments at room temperature.

F (MV/cm)	J_E (A/cm^2)	Condition
15	0	Piecewise desorption from apex
15	0.07	Piecewise desorption from apex
20	0	Coating removed from apex
20	0.07	Coating removed from apex
20–70	0	Piecewise desorption from shank
20–70	0.07	Piecewise desorption from shank

TABLE III. Summary of experiments at elevated temperatures.

F (MV/cm)	T (°C)	Condition
6.1	247	No change in LiF coating
6.1	380	Piecewise desorption from apex
6.1	470	Coating removed from apex
0	830	No change in LiF coating
3.9	830	Piecewise desorption from apex

first from the tip apex and then from the shank as a function of field strength. However; unlike the room temperature experiments, very small pieces of the coating (~5 nm) could be successively removed as the field was increased until the entire coating had been removed. The field required to cause piecewise removal of the coating was noticeably reduced at elevated temperatures. Unlike the room temperature experiments, a residual layer of LiF did not remain at the tip at elevated temperatures and higher field strengths. The results of the room temperature experiments are summarized in Table III.

IV. DISCUSSION

The removal of the LiF coating at any temperature (viz., pieces abruptly removed as the field is increased) is not characteristic of true field desorption, a process that occurs smoothly and gently as a function of field strength.[11] Instead, the removal of the coating is reminiscent of field-induced fatigue stress, a process that can be observed at the atomic level by field-ion microscopy.[12] Field-induced fatigue stress is known to initiate subgrain boundary development in perfect crystals, and can lead to shear components along slip planes that will often result in lattice destruction. The LiF coating on the tip apex is composed of numerous individual crystallites resulting in a coating that is inherently weaker than a bulk crystal. Dielectric breakdown of the LiF coating is unlikely, at least at room temperature where the breakdown field inside the coating will not be reached.[13] Since the removal process appears visually to be independent of temperature, it is highly probable that a single mechanism is responsible for the removal of a LiF coating from the apex of a field-emitter tip.

Field-induced fatigue stress is consistent with the magnitude of the electrostatic field stress induced at the coating in fields greater than 1 MV/cm. The field stress results from the energy density stored in the field whose magnitude $P = \epsilon_0 F^2/2$, where ϵ_0 is the permittivity of free space. If the field is expressed in MV/cm, the corresponding electrostatic pressure exerted on the coating (and directed outward from the tip apex) is

$$P(\text{lb/in.}^2) = 6F^2.$$

At room temperature, the field stress applied to the LiF coating is of the order of a half ton per in.^{2}. This is consistent with the range of mechanical yield strengths measured for this material.[14] At higher temperatures the yield strength will decrease, but the field required to remove the coating at el-

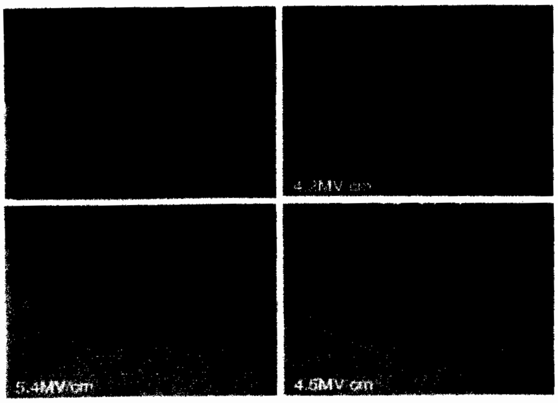

FIG. 6. Videotaped images showing the removal of lithium fluoride from the apex of a field-emitter tip as a function of tip bias, at a constant temperature of 830 °C. The electric field strength corresponding to the voltage displayed in the image was calculated using κR for the bare tip apex. The image magnification of the TV system used to record these images was not directly measured, but the thickness of the LiF coating was judged similar to that shown in Fig. 5.

evated temperatures also decreases. Field-induced fatigue stress appears to be the dominant mechanism for removal of LiF coatings in electrostatic fields.

V. ION PRODUCTION

Although ion currents were not monitored during the TEM experiments, the piecewise removal of the coating that is observed is unlikely to correspond to a significant ion yield. Experiments at room temperature have shown that no ion current is produced when LiF coatings on field-emitter tips are subjected to dc field strengths below 50 MV/cm.[13] The field strength required to remove a LiF coating is significantly higher when 20 ns voltage pulses are applied to the tip.[15] The pulsed experiments have further concluded:

> "that field desorption of Li^+ from intact LiF coatings is not possible using LiF coated metal anodes at room temperature. For ... thin films [$\leqslant$500 Å] field-stress-induced removal of the LiF coating occurs before fields necessary for ion formation are achieved. Subsequent emission of Li^+ occurs from LiF residue on the anode surface. With thick films [$\geqslant$100 nm] catastrophic vacuum arcs are initiated prior to the onset of any controllable ion emission process."[15]

The pulsed experiments are consistent with the TEM results presented above and further suggest that Li^+ production is not associated with piecewise removal of lithium fluoride coatings in electrostatic fields. This may have important, practical consequences for understanding and optimizing ion production in particle beam fusion accelerators (such as PBFA II) that use an anode coating of LiF to produce intense Li^+ ion beams. It is not unreasonable to expect that pieces of LiF could be abruptly torn from the anode surface as a pulsed electric field is generated. Enhanced electrical conductivity of the coating and the pieces (resulting from electron bombardment of a few hundred A/cm^2 during the voltage pulse) could facilitate ion production by the usual field-desorption mechanism.[16] Consequently, it seems imperative to determine experimentally if the anode coating in PBFA II is being disrupted by field-induced fatigue stress during the applied voltage pulse.

ACKNOWLEDGMENTS

This research was supported by Sandia National Laboratories under Contract No. AG-3854. The author gratefully acknowledges the interest and the expertise provided by Regan Stinnett of Sandia National Laboratories and T. A. Green (who participated in the imaging experiments). Tom Headley of Sandia National Laboratories provided TEM support for this study. Without Tom Headley's dedication and his willingness to try new approaches to TEM imaging, this experiment could not have been conducted.

[1]F. W. Röllgen and H. R. Schulten, Z. Naturforsch. **30**, 1685 (1975).
[2]F. W. Röllgen *et al.*, Z. Naturforsch. Teil A **31**, 1729 (1976).
[3]F. Okuyama *et al.*, Surf. Sci. **151**, L131 (1985).
[4]R. A. Gerber, in *The Physics and Technology of Ion Sources*, edited by I. G. Brown (Wiley, New York, 1989).
[5]P. F. McKay *et al.*, Rev. Sci. Instrum. **61**, 559 (1990).
[6]E. W. Müller and T. T. Tsong, *Field Ion Microscopy: Principles and Applications* (Elsevier, New York, 1969).
[7]Electro-Glo 300, a product of The Electro-Glo Company, 621 S. Kolmar Avenue, Chicago, IL, 60624.
[8]J. L. Boling and W. W. Dolan, J. Appl. Phys. **29**, 556 (1958).
[9]R. Gomer, *Field Emission and Field Ionization* (Harvard University Press, Cambridge, MA, 1961), p. 47.
[10]A. Klug, Chem. Scr. **14**, 291 (1978–9).
[11]E. W. Müller, Phys. Rev. **102**, 618 (1956).
[12]E. W. Müller, *Field Ionization and Field Ion Microscopy*, Advances in Electronics and Electronic Physics, Vol. 13 (Academic, New York, 1960), p. 83.
[13]A. L. Pregenzer *et al.*, J. Appl. Phys. **67**, 7556 (1990).
[14]E. Gillam, *Materials Under Stress* (Chemical Rubber, Boca Raton, FL, 1969); J. J. Gilman and W. G. Johnson, in *Solid State Physics*, Advances in Research and Applications, Vol. 13, edited by F. Seitz and D. Turnbull (Academic, New York, 1962), p. 148.
[15]P. R. Schwoebel and J. A. Panitz, J. Appl. Phys. **71**, 2151 (1992).
[16]T. A. Green *et al.*, Sandia National Laboratories Internal Report, 1994.